

# Passively Q-switched 1.57- $\mu\text{m}$ intracavity optical parametric oscillator

Yuri Yashkir and Henry M. van Driel

We demonstrate an eye-safe KTP-based optical parametric oscillator (OPO) driven intracavity by a diode-pumped 1064-nm Nd:YAG laser, passively Q-switched by a Cr<sup>4+</sup>:YAG crystal. The characteristics of this system, which operates at 1570 nm with a repetition rate as high as 50 Hz, are studied as a function of Cr<sup>4+</sup>:YAG optical density. Under optimum conditions the OPO generates 1.5-mJ,  $3.4 \pm 0.1$ -ns pulses in a single transverse mode. For a Cr<sup>4+</sup>:YAG Q-switch element with an optical density of 0.5 the conversion efficiency of the intracavity energy is  $\sim 45\%$  with the ratio of OPO to Nd:YAG peak-pulse intensity exceeding unity. These and other OPO characteristics compare favorably with a simple rate equation model of the OPO dynamics. © 1999 Optical Society of America

OCIS codes: 190.4970, 140.0140, 140.3540.

## 1. Introduction

The current interest in efficient, eye-safe coherent light sources for range finders and other applications has stimulated much interest in intracavity optical parametric oscillators (OPO's) driven by diode-pumped Nd<sup>3+</sup>:YAG lasers.<sup>1</sup> Although intracavity OPO's have been studied for nearly 30 years,<sup>2,3</sup> only recently, through the availability of high-damage-threshold crystals with favorable linear and nonlinear optical properties, such as KTiPO<sub>4</sub> (KTP), and stable, compact diode-pumped lasers have the merits of intracavity OPO's been really noted. Such all-solid-state systems take advantage of high intracavity laser intensity to allow an OPO to operate with a low threshold and high efficiency. Several such systems producing nanosecond pulses have been investigated experimentally.<sup>1,4-7</sup> Many of the OPO's use a 1064-nm Nd:YAG pump laser and typically an active Q-switch optical element. However, the inherent simplicity of passive Q switching has stimulated the development of solid-state saturable-absorber Q-switch elements. One such material, Cr<sup>4+</sup>:YAG, has been found to be particularly suitable for use in

Nd:YAG lasers.<sup>8</sup> A KTP OPO intracavity of a diode-pumped Nd:YAG laser used such a Q switch to produce 1570-nm signal pulses with a pulse energy of  $\sim 1$  mJ at a repetition rate of 1 Hz.<sup>7</sup> However, many details of this system are not known including the dependence of output pulse properties on saturable-absorber characteristics. In this paper we describe results of a systematic study of the dynamics of a KTP-OPO pumped intracavity by a Cr<sup>4+</sup>:YAG, Q-switched, diode-pumped, Nd<sup>3+</sup>:YAG laser. Debuisschert *et al.*<sup>9</sup> carried out extensive numerical simulations for an intracavity OPO considered to be continuously pumped by laser diodes and repetitively Q switched at a variable rate by an unspecified mechanism. We extend this model to the specific case in which Q switching is induced by a passive, saturable-absorber element. The overall model is able to reproduce the salient features of the OPO operation.

## 2. Intracavity Optical Parametric Oscillator

### A. Experiment

A schematic diagram of our OPO is shown in Fig. 1. The active laser medium consists of an antireflection coated Nd:YAG rod (1.1% Nd<sup>3+</sup> doping, 40-mm length, 2-mm diameter), side-pumped by pulses of energy up to 120 mJ from three two-bar stacked diode arrays emitting at 810 nm at a repetition rate<sup>10</sup> as high as 50 Hz. The diode pulses are 200  $\mu\text{s}$  long to match closely the upper laser level lifetime of 230  $\mu\text{s}$ . The 30-cm-long laser cavity was formed by two high (0.998) reflectors at the OPO pump wavelength of  $\lambda_p = 1064$  nm ( $M_1$  is a flat mirror and  $M_3$  is a spherical

The authors are with the Department of Physics, University of Toronto, 60 St. George Street, Toronto, Ontario M5S 1A7, Canada. The e-mail address for H. M. van Driel is vandriel@physics.utoronto.ca.

Received 2 November 1998; revised manuscript received 9 December 1998.

0003-6935/99/122554-06\$15.00/0

© 1999 Optical Society of America

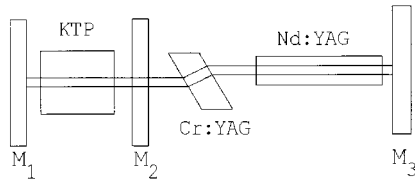


Fig. 1. Intracavity OPO configuration:  $M_1$ , flat output coupler for  $[0.75 < R_S < 0.95$  at  $\lambda_S = 1570$  nm, HR (high reflectivity) at 1064 nm];  $M_2$ , black mirror of OPO cavity (HR at 1570 nm, high transmissivity at 1064 nm);  $M_3$ , spherical back mirror of pump laser cavity (HR at 1064 nm).

mirror with a radius of curvature of 5 m). For passive  $Q$ -switched operation the cavity contained a Brewster-oriented  $\text{Cr}^{4+}$ :YAG crystal plate; plates with optical densities (OD's) of 0.2, 0.3, and 0.5 and thicknesses of 2–5 mm were used. The 6-cm-long OPO cavity contained a 5.5 mm  $\times$  5.5 mm  $\times$  25 mm KTP crystal cut at  $\theta = 90^\circ$  and  $\phi = 0^\circ$  and placed with the  $x$  axis along the axes of the cavity to yield type II ( $o \Rightarrow o + e$ ) noncritical phase matching for a signal wavelength of  $\lambda_S = 1570$  nm; the crystal was antireflection coated for this wavelength. The OPO cavity was formed by a flat high reflector,  $M_2$  (for  $\lambda_S = 1570$  nm), and a flat output coupler,  $M_1$ , with reflectivity  $0.75 < R_S < 0.95$ . The pump wave polarization, defined by the Brewster-oriented  $\text{Cr}^{4+}$ :YAG crystal, was oriented along the  $y$  axis of the KTP crystal.

### B. Rate Equation Model

To assist our understanding of the operation of the passively  $Q$ -switched laser/OPO combination, we have considered an extension of the simple rate equation model for repetitively  $Q$ -switched systems developed by Debuisschert *et al.*<sup>9</sup> The dynamic optical variables are taken to be the intracavity intensities of pump  $I_P(t)$  and signal  $I_S(t)$  pulses, which are defined here to be normalized by the pump intensity at the threshold for the OPO. These variables are considered along with the population inversion in the  $\text{Nd}^{3+}$ :YAG crystal  $N(t)$  normalized by its value at the threshold of the pump laser and the population of the ground level of the  $\text{Cr}^{4+}$ :YAG saturable absorber  $N_C(t)$  normalized by its unperturbed value. For the pump beam intensity one has

$$\tau_p \frac{dI_P}{dt} = N(I_P + \epsilon) - I_P(1 + \alpha N_C + fI_S), \quad (1)$$

where  $\tau_p$  is the pump cavity photon lifetime. The first term on the right-hand side corresponds to stimulated emission and spontaneous emission (through parameter  $\epsilon$ ) whereas the second term represents losses due to cavity lifetime effects, attenuation at the saturable absorber, and signal pulse conversion. For the signal beam intensity we have

$$\tau_s \frac{dI_S}{dt} = I_P(I_S + \epsilon') - I_S, \quad (2)$$

where  $\tau_s$  is the OPO photon cavity lifetime. The first term on the right-hand side represents stimulated emission due to pump and noise photons (represented by  $\epsilon'$ ), and the second term is associated with OPO cavity losses. The relative finesse of the OPO and the pump cavity is defined by the parameter  $f = (1 - R_S')/(1 - R_P')$ , where  $(1 - R_S')$  and  $(1 - R_P')$  represent (reflection, scattering, absorption) losses for signal and pump cavities, respectively.

The corresponding equations for the two population variables are

$$\tau_N \frac{dN}{dt} = \sigma - N(1 + xI_P), \quad (3)$$

$$\tau_{N_C} \frac{dN_C}{dt} = 1 - N_C(1 + \beta I_P), \quad (4)$$

where  $\tau_N$  and  $\tau_{N_C}$  are the lifetimes of the active media and saturable-absorber excited states. The pumping level of the active laser media ( $\text{Nd}^{3+}$ :YAG) is defined by parameter  $\sigma$ . (For the non- $Q$ -switched laser case,  $\sigma = 1$  corresponds to the laser threshold.) The parameter  $x$  is the ratio of the OPO threshold to the saturation limit of the laser medium. Absorption of the pump light in the saturable absorber is described by parameter  $\alpha$ , which is defined so that  $\tau_p/(1 + \alpha)$  is the lifetime of the pump photons when the saturable absorber is at its ground level ( $N_C = 1$ ). The parameter  $\beta$  is the ratio of the OPO threshold to the saturation limit of the saturable absorber. Equations (1)–(3) are identical to those used by Debuisschert *et al.* except that Eq. (1) contains the specific loss mechanism associated with the saturable absorber  $Q$  switch. Equation (4) is introduced here to account for the specific dynamics of the passive  $Q$  switch.

Below we consider the solution of these equations by using initial conditions  $I_P(0) = I_S(0) = N(0) = 1 - N_C(0) = 0$ . The emphasis is on obtaining a semi-quantitative description of the laser and OPO dynamics. No explicit attempt is made to obtain absolute numbers for beam intensities and energies. These amplitude variables are extremely sensitive to the parameters in the model. For the simulations we use the usual material parameters,  $\tau_N = 200$   $\mu\text{s}$  (Ref. 11) and  $\tau_{N_C} = 8.5$   $\mu\text{s}$  (Ref. 12), and the parameters  $\tau_p = 20$  ns and  $\tau_S = 1.8$  ns, as determined for our laser/OPO by using the expressions given by Debuisschert.<sup>9</sup> We also choose  $\epsilon = \epsilon' = 10^{-5}$  to initiate laser/OPO operation; the results of the simulations are not very sensitive to these values. The  $x$ ,  $\beta$ , and  $\sigma$  are defined below when we consider comparisons of the numerical simulations with experimental results.

### 3. Results and Discussion

We consider first the operation of the  $Q$ -switched laser/OPO as a function of diode-pumped laser pulse energy  $E_D$ . The individual output pulse characteristics did not change significantly for repetition rates as high as 50 Hz. For all the results reported here the repetition rate used is 15 Hz. Well above the laser threshold of approximately  $E_D = 43$  mJ (for an

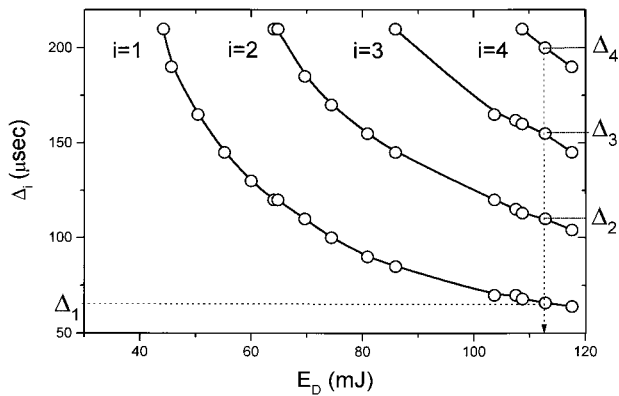


Fig. 2. Dependence of time shift  $\Delta_i$  of nanosecond pulses ( $i = 1, 2, \dots$ ) generated in a passively  $Q$ -switched laser cavity on diode pulse energy  $E_D$ :  $Q$ -switch element optical density, OD = 0.2.

OD = 0.2  $Q$  switch) a sequence of nanosecond signal pulses is generated within each laser-diode pulse. Such repetitive  $Q$  switching has also been reported for cw-pumped laser systems employing a  $\text{Cr}^{4+}$ :YAG saturable absorber.<sup>13</sup> In Fig. 2 the time of generation for the  $i$ th pulse  $\Delta_i$  (measured with respect to the front edge of the diode-pumped pulse) is shown as a function of  $E_D$  in the case of an OD = 0.2  $\text{Cr}^{4+}$ :YAG absorber. An additional pulse appears when  $E_D$  increases by approximately 20 mJ. This energy is lower than that required for the threshold to be reached for the first pulse since there is still considerable population in the upper laser level after emission of a  $Q$ -switched pulse.<sup>9</sup> One can estimate the stored energy utilization factor as  $<0.5$ , implying that the ratio of inversion before  $Q$  switching to threshold inversion is<sup>14</sup>  $\sigma < 1.5$ . The time delay  $\Delta_t$  between pulses is approximately constant. (For a total diode-laser-pulse energy of 112 mJ it is  $\Delta_t = 45 \pm 2 \mu\text{s}$ .)

In Fig. 3 the oscilloscope traces of diode pulses and nanosecond signal pulses corresponding to Fig. 2 are shown in conditions in which the total diode-pumped

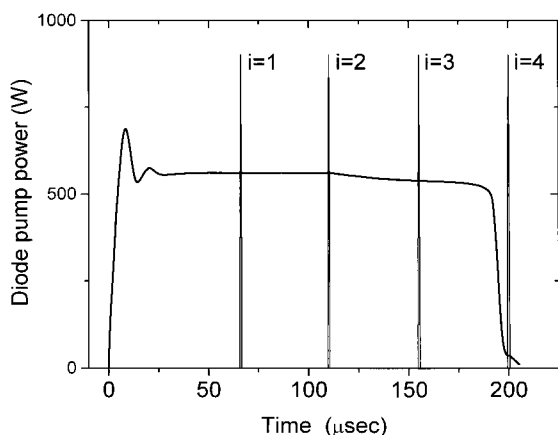


Fig. 3. Oscilloscope traces of diode pulse power and nanosecond pulses at a diode pulse pump of energy of 112 mJ and a  $Q$  switch of OD = 0.2.

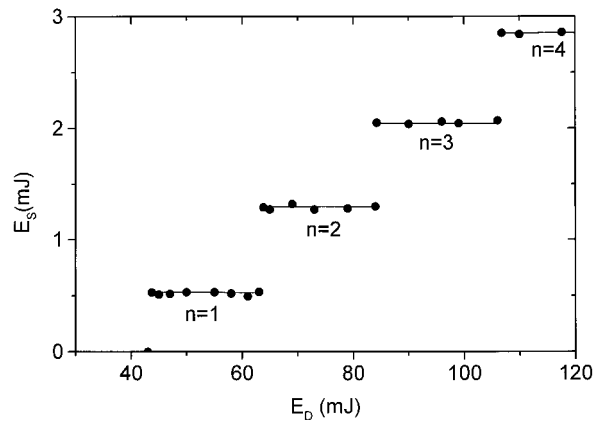


Fig. 4. Signal-pulse energy versus diode-pulse energy for a  $Q$ -switch optical density of OD = 0.2.

energy is 112 mJ. Obviously for a  $\text{Cr}^{4+}$ :YAG saturable absorber with a higher OD, at a given diode-pumped energy the time shift  $\Delta_1$  (and delays  $\Delta_{i+1} - \Delta_i$ ) increases since the threshold for  $Q$ -switched action is raised, and more time is needed to store the necessary amount of energy in Nd:YAG. For a sufficiently high value of OD only one laser pulse is generated for  $E_D = 120$  mJ. For this energy and an OD = 0.3  $Q$ -switch element we were able to obtain three pulses, whereas the OD = 0.5 element gave us only one pulse approximately 150  $\mu\text{s}$  after the beginning of the diode laser pulse.

In Fig. 4 the dependence of energy  $E_S$  of the 1570-nm signal pulses is shown as a function of  $E_D$  for an OD = 0.2 saturable absorber. The threshold of  $Q$ -switched laser operation is reached at  $E_D \sim 43$  mJ, as also indicated in Fig. 2, at the end of the diode pulse. This laser-diode-pulse energy yields a signal pulse with an energy of  $\sim 0.5$  mJ. Increasing  $E_D$  does not increase the energy of the 1064-nm laser pulse or of the OPO pulses, since the saturable absorber is bleached at a certain constant energy inside the cavity and this energy is not reached again during the diode laser pulse. However, for a sufficiently high  $E_D$  the threshold of bleaching is reached again within a laser diode pulse and the appearance of additional pulses results in a steplike increase in the total energy as seen in Fig. 4. An analogous dependence of laser output energy was observed by Lavi *et al.*<sup>5</sup> This type of self-locking,  $Q$  switching is in the nature of passive  $Q$  switches.

For OD values higher than 0.2 the bleaching of the passive  $Q$ -switching element occurs later in the diode pulse, thus enabling the laser medium to store more energy before release. As a result the energy  $E_P$  of the laser pulse and corresponding OPO signal pulse energy  $E_S$  increases as the OD increases. The signal pulse energy per emitted pulse was measured for the three available saturable absorbers (OD = 0.2, 0.3, and 0.5) as shown in Fig. 5. Although there are only three data points it appears that across the range of OD's considered the dependence of  $E_S$  on saturable-absorber transmissivity ( $T = 10^{-\text{OD}}$ ) is not far from

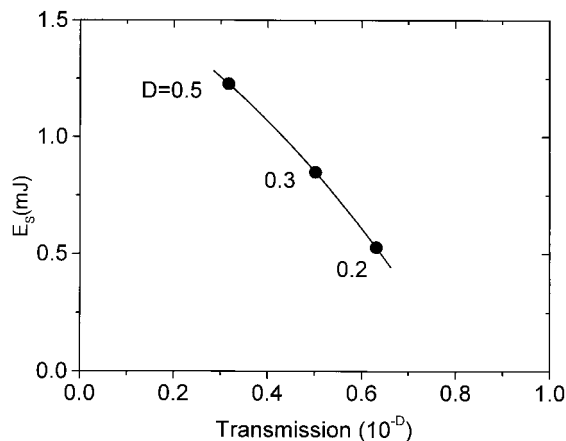


Fig. 5. Average energy of a single signal pulse generated with different passive  $Q$ -switching elements ( $OD = 0.2, 0.3, 0.5$ ) versus transparency ( $=10^{-OD}$ ).

linear. The effect of the increasing  $OD$  is therefore to reduce the number of pulses, to increase the energy per pulse, but not to improve the energy utilization factor significantly.

The optimum output efficiency of the 1064-nm laser and the OPO ( $OD = 0.5$   $Q$  switch) can be determined separately by varying the reflectivity of the appropriate mirrors. The variation of laser and signal energy with reflectivity of the output coupler is indicated in Fig. 6. In the first case the system was used in normal OPO operation with a different output coupler  $M_1$  reflectivity at  $\lambda_S$  (but highly reflecting at  $\lambda_P$ ). In the second case the system was used with mirror  $M_2$  slightly tilted to prevent OPO operation and with a variable 1064-nm output coupler ( $M_1$ ). Optimal output couplers were found to have  $R_P = 0.4$  for the second case (corresponding to a maximum laser pulse energy of 3.6 mJ) and  $R_S = 0.85$  for OPO operation. (The maximum signal pulse energy is 1.42 mJ.) Note that the ratio of the maximum OPO signal pulse energy to the maximum 1064-nm pulse energy (albeit for different cavity configurations) is

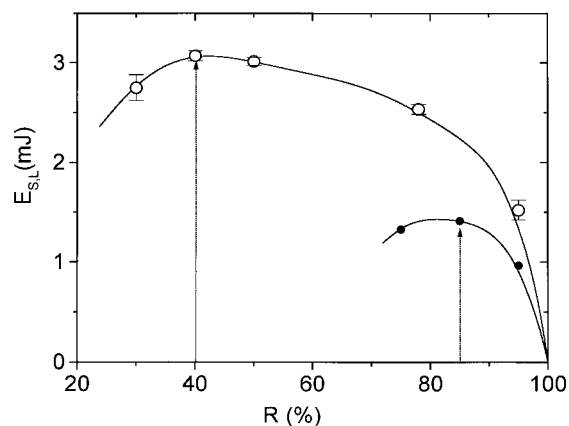


Fig. 6. Dependence of the output energy of the  $Nd^{3+}$ :YAG laser (open circles) and OPO signal (solid circles) on the reflectivity of the output coupling mirror.

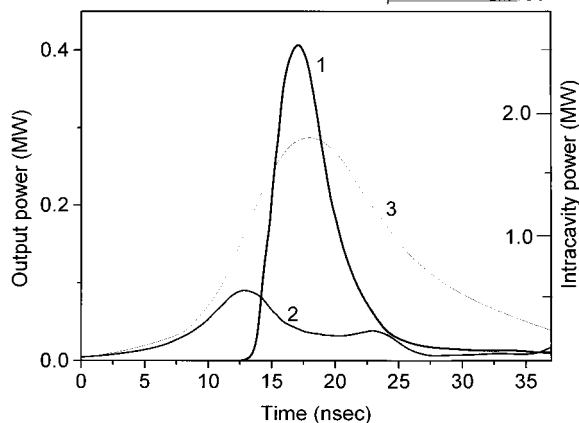


Fig. 7. Temporal shape of pulses generated in  $OD = 0.5$  case: 1, output OPO signal pulse generated with optimal output coupling for 1570 nm; 2, output laser pulse generated with optimal output coupling for 1064 nm; 3, intracavity laser pulse during OPO optimal operation. (For intracavity power of pulses 1 and 3 use the right-hand scale.)

$\sim 0.4$  for our pumping conditions. Debuisschert *et al.*<sup>9</sup> estimated that this ratio could be as high as 0.8.

We consider now the temporal dynamics of the laser and OPO signal pulses for  $OD = 0.5$  operation with  $E_D = 112$  mJ. Oscilloscope traces of typical pulses are shown in Fig. 7. In the figure pulses 1 and 2 are obtained with a closed cavity at  $\lambda_P$  and optimal output coupling ( $R_S = 0.85$ ) for the intracavity OPO. Pulse 3 is recorded when the laser is configured ( $M_2$  is tilted) to produce the maximum 1064-nm output energy. Owing to the high efficiency of the OPO, the intracavity laser pump power is very low (this power was obtained by detecting the 1064-nm pulse leakage from mirror  $M_3$ ) when an OPO pulse is obtained and there is strong depletion of the laser pulse during the signal-pulse generation. Under optimal conditions the width of the signal pulse was determined to be  $\tau_S = (3.4 \pm 0.1)$  ns, a value related to the bare cavity photon lifetime of  $\sim 1.8$  ns. Debuisschert *et al.* predicted a ratio of the pulse width to the cavity photon lifetime of  $\sim 3$ , which compares favorably with our value of 1.9. Longer pulses are obtained under less ideal conditions (e.g., lower  $E_D$ , higher coupler reflectivity).

The relatively short signal pulse indicates that the OPO effectively cavity dumps the laser energy. The intracavity energy conversion efficiency from 1064 to 1570 nm is  $\sim 0.45$  (defined as the intracavity signal-pulse energy divided by total intracavity energy) and is within 20% of the theoretical value calculated by Debuisschert *et al.* This efficiency is approximately the same as the ratio of the maximum 1570-nm to the maximum 1064-nm pulse energies as noted above) although the ratio of peak pulse powers is  $>1.5$ . This peak-power enhancement is simply a result of the nonlinear optical generation process in a short OPO cavity. Note, however, that both the 1064- and the 1570-nm pulses possess a tail since the laser is never far from threshold toward the end of the

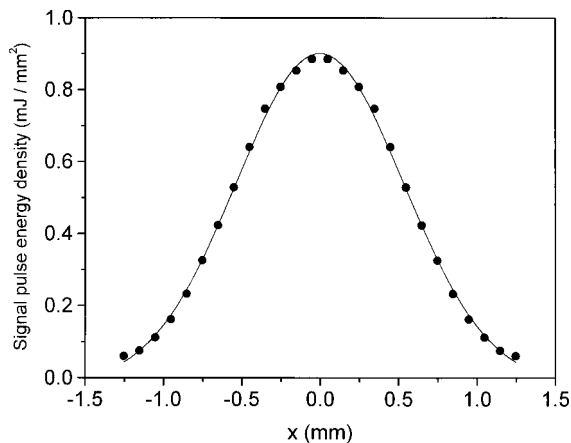


Fig. 8. Spatial profile of output signal beam:  $x$ , transverse coordinate; circles, experimental points; curve, best Gaussian fit.

$Q$ -switched pulse. The ratio of rise and fall times in our signal pulse is 0.77, which compares favorably with a value of 0.72 determined by Debuisschert *et al.* From Fig. 7 we also infer that the ratio of the peak intracavity 1570- and 1064-nm powers is 4.4 compared with a theoretical value of 4.5. Finally, Fig. 8 illustrates the transverse mode of the signal beam and indicates that a high-quality smooth profile is obtained. Owing to the saturable-absorber element that works as a soft diaphragm, the output beam mode structure is essentially Gaussian.

We now consider specific aspects of the passively  $Q$ -switched laser performance compared with the results predicted by the rate equations outlined above. The parameters used in the simulation are  $f = 1$ ,  $x = 2 \times 10^3$ ,  $\beta = 10^3$ , which are obtained by using the expressions of Debuisschert *et al.* and the cavity losses, beam waists, material saturation intensities of the Nd:YAG and Cr<sup>4+</sup>:YAG media. We use a laser pumping level of  $\sigma = 12$ , which is consistent with experiments. Numerical results from the simulations do not change substantially if the  $x$  or  $\beta$  parameters are changed by as much as a factor of 2. When the diode pump is turned on, the active medium population grows at a rate of  $\sigma/\tau_N$  and after several microseconds reaches the threshold for stimulated emission. At that time the pump intensity grows exponentially at a rate of  $(N - 1 - \alpha)/\tau_p$ . Simultaneously the saturable-absorber ground-state population  $N_c$  decreases at a rate of  $\beta I_p/\tau_{N_c}$  and on a time scale of nanoseconds is bleached ( $N_c = 0$ ). Note that, unlike the case discussed by Debuisschert *et al.*, passive  $Q$  switching requires a nonzero buildup time. When the pump pulse intensity  $I_p$  reaches the threshold for OPO operation ( $I_p = 1$ ), the analogous exponential growth of signal radiation starts from noise level  $\epsilon$ . The time rate of OPO generation is high enough [ $(I_p - 1)/\tau_S$ ] to dump the pump energy efficiently. As a result, nanosecond-duration pump and signal pulses are generated as indicated in Fig. 9. When one compares these simulations, based on  $\alpha = 7$ , with the experimental pulses shown in Fig. 7, good

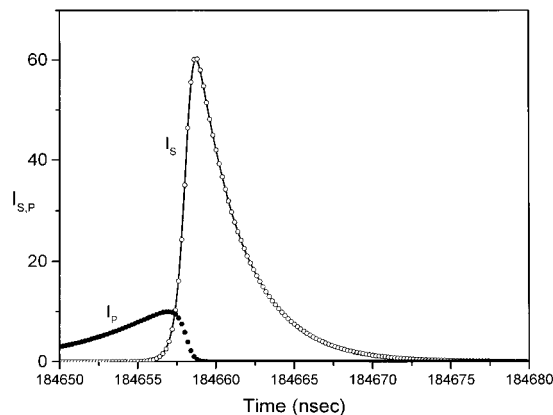


Fig. 9. Time-dependent pump intensity  $I_p$  (solid circles) and OPO signal intensity  $I_s$  (open circles) obtained with a saturable absorber with  $\alpha = 7$ . Time is measured from the turn-on of the diode laser pump.

semiquantitative agreement is obtained. The signal pulse has an intracavity intensity that is much larger than that of the laser pulse, and its duration of 3 ns is considerably less than that of the laser pulse.

The simulations show that the generation of pump and signal pulses occurs at a time that increases close to linearly with the OD of the saturable absorber (parameter  $\alpha$ ), varying from 40  $\mu$ s for  $\alpha = 1$  to 180  $\mu$ s for  $\alpha = 7$ . As  $\alpha$  (which is proportional to  $10^{-OD}$ ) increases the signal pulses become shorter but have higher peak intensity and energy. Figure 10 illustrates how the signal-pulse profile varies with  $\alpha$ . Figure 11 offers a summary of how the signal-pulse width, peak intensity, and energy vary with the unsaturated absorption of the absorber. Note, in particular, that the pulse width is only weakly dependent on  $\alpha$  for  $\alpha > 2-3$ , but that the peak intensity and signal-pulse energy grow almost linearly with  $\alpha$ . The pulse energy variation, in particular, agrees well with the experimental data in Fig. 5.

The main conclusion from the simulation is that, for a given laser-diode pumping level, one should use the highest OD of the saturable absorber possible so that

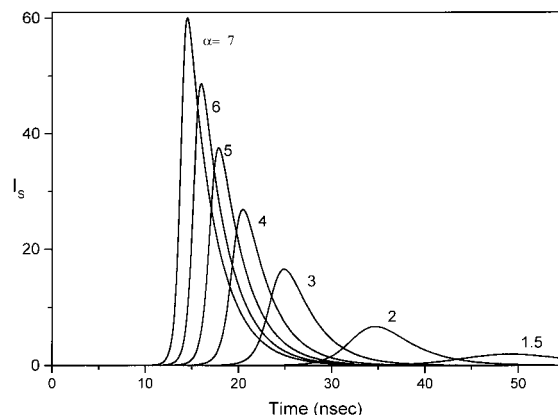


Fig. 10. Time-dependent signal pulses for a given  $\alpha$ . At  $t = 0$  the pump intensity is  $I_p = 1$  (the threshold of OPO).

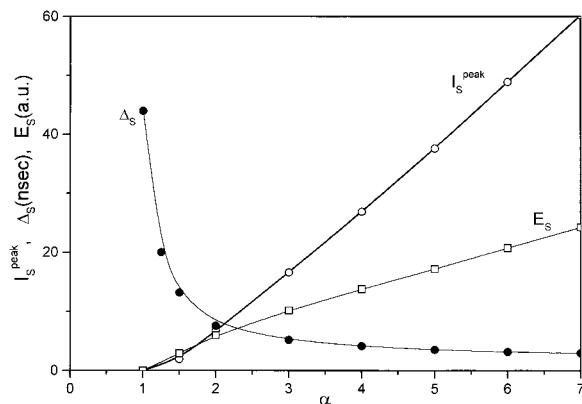


Fig. 11. Peak intensity  $I_p$ , pulse energy  $E_s$ , and pulse width  $\Delta_s$  of signal pulses versus saturable-absorber density parameter  $\alpha$ .

the OPO signal pulse occurs as close to the end of the diode pulse, with maximum intensity and energy.

#### 4. Conclusions

We have studied the dynamics and the pulse characteristics of a noncritically phase-matched, KTP-based OPO-driven intracavity by a laser-diode side-pumped Nd:YAG laser passively  $Q$  switched by a  $\text{Cr}^{4+}$ :YAG crystal. We obtained high-efficiency OPO operation owing to high intracavity-energy-transfer efficiency. The OPO energy, pulse, and efficiency characteristics are in good agreement with theoretical modeling based on an extension of the model of Debuisschert *et al.*,<sup>9</sup> taking into account that we have employed a passive  $Q$  switch. The use of passive  $Q$  switching permits a simple system to be constructed, and the use of an appropriate saturable-absorber element allows one signal pulse to be generated per diode laser pulse. However, the trade-off is that such an element must generate a high loss in the off-state. This limits the energy-transfer efficiency from the laser gain medium.

We gratefully acknowledge financial support from the Natural Sciences and Engineering Research Council of Canada, Photonics Research Ontario, and Hughes-Elcan, Midland, Ontario.

#### References and Notes

1. See, for example, *Advanced Solid State Lasers*, W. R. Bosenberg and M. M. Feyer, eds., Vol. 19 of OSA Trends in Optics and Photonics Series (Optical Society of America, Washington, D.C., 1998).
2. M. K. Oshman and S. E. Harris, "Theory of optical parametric oscillation internal to the laser cavity," *IEEE J. Quantum Electron.* **QE-4**, 491–502 (1968).
3. J. Falk, J. M. Yarborough, and E. O. Amman, "Internal optical parametric oscillation," *IEEE J. Quantum Electron.* **QE-7**, 359–369 (1971).
4. L. R. Marshall, A. D. Hays, J. Kasinski, and R. Burnham, "Highly efficient optical parametric oscillators," in *Eye-Safe Lasers: Components, Systems, and Applications*, A. M. Johnson, ed., Proc. SPIE **1419**, 141–152 (1991).
5. R. Lavi, A. Englander, and R. Lallouz, "Highly efficient low-threshold tunable all-solid-state intracavity optical parametric oscillator in the mid infrared," *Opt. Lett.* **21**, 800–802 (1996).
6. A. R. Geiger, H. Hemmati, W. H. Farr, and N. S. Prasad, "Diode-pumped optical parametric oscillator," *Opt. Lett.* **21**, 201–203 (1996).
7. P. Ketteridge, I. Lee, M. Gagnon, W. Radcliff, and E. Chicklis, "Miniature eyesafe range finder," in *Conference on Lasers and Electro-Optics*, Vol. 15 of 1995 OSA Technical Digest Series (Optical Society of America, Washington, D.C., 1995), p. 257.
8. Y. Shimony, Z. Burshtein, and Y. Kalisky, " $\text{Cr}^{4+}$ :YAG as passive  $Q$ -switch and Brewster plate in a pulsed Nd:YAG laser," *IEEE J. Quantum Electron.* **31**, 1738–1741 (1995).
9. T. Debuisschert, J. Raffy, J.-P. Pocholle, and M. Papuchon, "Intracavity optical parametric oscillator: study of the dynamics in pulsed regime," *J. Opt. Soc. Am. B* **13**, 1569–1587 (1996).
10. This laser is similar to a system described by U. J. Greiner, H. H. Klingenberg, D. R. Walker, C. J. Flood, and H. M. van Driel, "Diode pumped Nd:YAG laser using reflective pump optics," *Appl. Phys. B* **58**, 393–395 (1994).
11. W. Koechner, *Solid State Laser Engineering*, 2nd ed. (Springer-Verlag, New York, 1988), p. 48.
12. *Union Carbide Corporation Data Notes* (Union Carbide Corporation, Danbury, Conn., 1996).
13. Y. Shimony, Z. Burshtein, A. Ben-Amar Baranga, Y. Kalisky, and M. Stauss, "Repetitive  $Q$  switching of a CW Nd:YAG laser using  $\text{Cr}^{4+}$ :YAG saturable absorbers," *IEEE J. Quantum Electron.* **32**, 305–310 (1996).
14. A. Yariv, *Quantum Electronics*, 3rd ed. (Wiley, New York, 1989), p. 534.